2016 International Symposium on Nonlinear Theory and Its Applications,
NOLTA2016, Yugawara, Japan, November 27th-30th, 2016

Common-signal-induced synchronization in photonic integrated circuits driven by constant-amplitude random-phase light

Takuma Sasaki[1], Izumi Kakesu[1], Atsushi Uchida[1],
Satoshi Sunada[2,3], Kazuyuki Yoshimura[1,4] and Kenichi Arai[2]

[1]Department of Information and Computer Sciences, Saitama University,
255 Shimo-Okubo, Sakura-ku, Saitama City, Saitama, 338-8570, Japan
[2]NTT Communication Science Laboratories, NTT Corporation
3-1 Morinosato, Wakamiya, Atugi-Shi, Kanagawa 243-0198, Japan
[3]Faculty of Mechanical Engineering, Kanazawa University,
Kakuma-machi, Kanazawa, Ishikawa 920-1192, Japan
[4]Department of Information and Electronics, Graduate school of Engineering, Tottori University
4-101 Koyama-Minami, Tottori 680-8552, Japan
Emails: s15mm312@mail.saitama-u.ac.jp, auchida@mail.saitama-u.ac.jp

Abstract—We experimentally and numerically investigate common-signal-induced synchronization in photonic integrated circuits (PICs) driven by constant-amplitude random-phase light. We measure the cross-correlation value between the outputs of the two PICs when the feedback phase is changed. The temporal waveforms of PICs show high cross-correlation when the feedback phases are matched, whereas low correlation is obtained when they are mismatched. The RF spectra of two PICs are similar to each other when the feedback phase is matched.

1. Introduction

Information-theoretic security [1] has been studied as a new information-security paradigm to replace the computational security. A private key distribution method has been proposed using correlated random bits as a key distribution based on information theory security [2–5]. This method generates a secret key from a random number sequence with a correlation that can be shared by two users. Common-signal-induced synchronization is a key technique for this method and has been demonstrated using semiconductor lasers [6–10]. It utilizes the phenomenon that the output waveforms of two lasers (called Response lasers) are synchronized by injecting a common drive laser output. Synchronization is achieved only when the phase parameters between the Response lasers are matched. However, synchronization is unstable in an optical-fiber-based system with long external cavity length (e.g., several meters) [8] because the optical phase fluctuates under the influence of air turbulence and temperature fluctuation.

In this study, we experimentally and numerically investigate common-signal-induced synchronization in photonic integrated circuits driven by constant-amplitude random-phase (CARP) light.

2. Experimental setup

The structure of the photonic integrated circuit used in this study is shown in Fig. 1. The output of the distributed-feedback (DFB) laser is reflected by an external mirror. The phase and intensity of the optical feedback is adjusted by a phase modulator (PM) and an optical amplifier (SOA), respectively. The optical output of the DFB laser can be detected through an optical fiber, and CARP light can be injected as well. The external cavity length is 8.6 mm, which corresponds to the external cavity frequency of 4.9 GHz. When the external cavity frequency is higher than the relaxation oscillation frequency, the laser is defined as short cavity regime (SCR). We set the injection current as $J = 1.2\ J_{th}$ for synchronization. In this case, the relaxation oscillation frequency is 1.8 GHz, which satisfies the condition of the short cavity regime with the PICs.

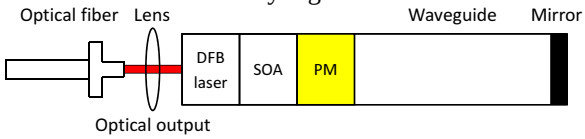

Figure 1: Schematics of the photonic integrated circuit. SOA, semiconductor optical amplifier; PM, phase modulator;

The experimental setup is shown in Fig. 2. We use a semiconductor laser (Drive) and two PICs (PIC 1, and PIC 2) for common-signal-induced synchronization. We generate an optical noise signal from the output of a superluminescent diode (SLD). The optical phase of the drive signal is modulated randomly by the output of the SLD to generate CARP light. The CARP light from the Drive laser is divided by a fiber coupler (FC). Each CARP light is injected into the PIC unidirectionally through an optical isolator (ISO). The injection strength of the CARP light is adjusted by an optical attenuator (ATT). The optical feedback of the PICs is controlled by the SOA current (called

closed-loop configuration). The phase of the optical feedback in each PIC is modulated by a waveform generator. The output waveforms of the CARP light and the two PICs are observed by photodetectors and amplified by electric amplifiers. The converted electrical signals are detected by using a digital oscilloscope and a radio-frequency (RF) spectrum analyzer.

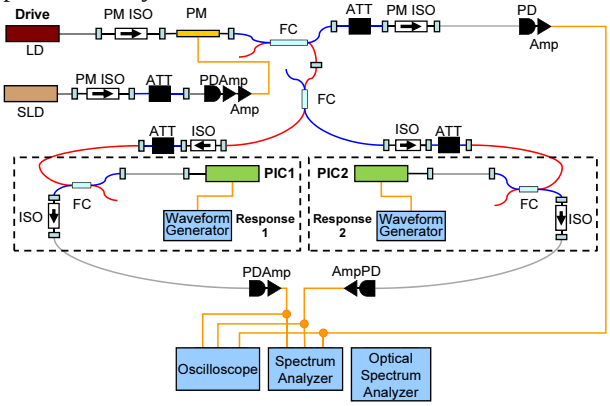

Figure 2: Experimental setup of common-signal-induced synchronization in two PICs with CARP light. Amp, electric amplifier; ATT, attenuator; FC, fiber coupler; ISO, optical isolator; PIC, photonic integrated circuit; PD, photodetector; PM, phase modulator; SLD, superluminescent diode.

3. Experimental results

We experimentally investigate common-signal-induced synchronization when the photonic integrated circuits are used as the Response lasers. We introduce a measure of cross-correlation to evaluate the quality of synchronization. The cross-correlation value is calculated as follows:

$$C = \frac{\langle (I_1 - \bar{I}_1)(I_2 - \bar{I}_2) \rangle}{\sigma_1 \cdot \sigma_2} \qquad (1)$$

where I_1, I_2 are the temporal waveforms of the output intensities of the PIC 1 and 2, respectively, $\bar{I}_1, \bar{I}_2$ are their mean values, σ_1, σ_2 are their standard deviations of I_1, I_2, and $< >$ is time averaging. $C = 1$ indicates identical synchronization, whereas $C = 0$ indicates no synchronization.

Figure 3 shows the temporal waveforms of the PIC 1 and 2 and their correlation plots. In Figs. 3(a) and (b), when the voltages of the PM are set to 0.0 V for both of the PICs, the temporal waveforms of the two PICs are strongly correlated. We obtain a high cross-correlation value of 0.932 as shown in Fig. 3(b). On the other hand, when the feedback phase is mismatched, the temporal waveforms of the two PICs are weekly correlated in Figs. 3(c) and (d). The cross-correlation shows a low value of 0.135 as shown in Fig.3(d). We thus experimentally achieve common-signal-induced synchronization of the two PICs with phase modulation.

Figure 4 shows the RF spectra of the PIC 1 and 2. $V_{PM1,2}$ denote the voltages applied to the PM of the PIC 1 and 2,

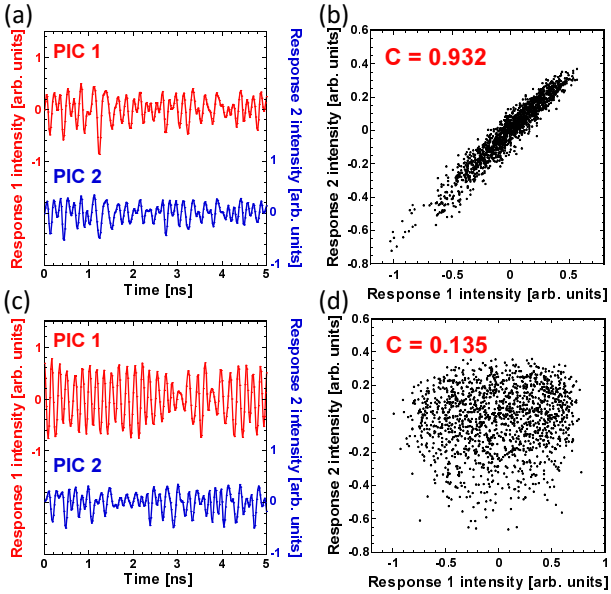

Figure 3: (a),(c) Temporal waveforms of PIC 1 and PIC 2, and (b),(d) correlation plots. The phases of the feedback lights are matched in (a),(b) and mismatched in (c),(d).

respectively. The feedback phases of the PICs are matched in Fig. 4(a), while they are mismatched in Fig. 4(b). The two RF spectra are in good agreement in Fig. 4(a) with the same parameter values of the feedback phases. We change the voltage of the PM of PIC 1 to 1.176 V in Fig. 4(b) and the two RF spectra are not matched. The change in the RF spectra is observed by varing the feedback phase in the short-cavity regime due to the large external cavity frequency of PICs (4.9 GHz).

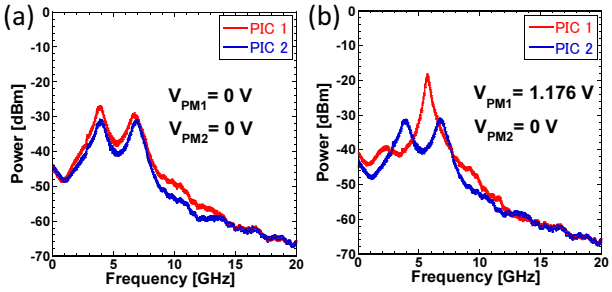

Figure 4: RF spectra of the PIC 1 and 2. The feedback phases of PICs are (a) matched, and (b) mismatched.

4. Numerical model

We conduct numerical simulations to reproduce our experimental results. We use the Lang-Kobayashi equations [11] to describe a model consisting of the PICs with CARP light injection as follows [7].

$$\begin{aligned} \frac{dE_r(t)}{dt} = & \frac{1+i\alpha}{2}\left[\frac{G_N(N_r(t)-N_0)}{1+\epsilon|E_r(t)|^2} - \frac{1}{\tau_p}\right]E_r(t) \\ & + \kappa_r E_r(t-\tau_r)\exp(i\omega_r\tau_r) \\ & + \sigma E_d(t-\tau_{inj})\exp[i(\Delta\omega t - \omega_r\tau_{inj})] \end{aligned} \qquad (2)$$

$$\frac{dN_r(t)}{dt} = J_r - \frac{N_r(t)}{\tau_s} - \frac{G_N(N_r(t)-N_0)}{1+\epsilon|E_r(t)|^2}|E_r(t)|^2 \quad (3)$$

$$E_d(t) = \sqrt{I(t)}\exp[i\varphi(t)] \quad (4)$$

Where, $E_r(t)$ and $N_r(t)$ are the electric field amplitude and the carrier density of the PICs. The CARP light is shown in Eq. (4) [7]. $\varphi(t)$ is generated by the stochastic differential equation based on the Ornstein-Uhlenbeck process. The fixed parameters are $r, G_N, N_0, \epsilon, \tau_p, \tau_s$, and α. They correspond to the gain coefficient, the carrier density at transparency, the gain saturation coefficient, the photon lifetime, the carrier lifetime, and the linewidth enhancement factor, respectively. The variable parameters are $\kappa, J, \tau, \sigma, \tau_{inj}, \omega$ and $\Delta\omega$. They correspond to the feedback strength, the injection current, the feedback delay time, the injection strength, the propagation delay time from the drive laser to the PICs, the optical frequency, and the optical frequency detuning between the drive laser and the PICs, respectively. In this study, we set the parameter values as follows: $\kappa = 10.9\,\mathrm{ns}^{-1}$, $J_r = 1.16\,J_{th}$, $\tau = 0.21$ ns, and $\sigma = 2.3\,\mathrm{ns}^{-1}$. $\Delta\omega$ describes $\Delta\omega = 2\pi\Delta f_{sol}$, where Δf_{sol} is the optical frequency detuning between Drive laser and PICs $\Delta f_{sol} = -4.0$ GHz.

5. Numerical results

Figure 5 shows the temporal waveforms and the cross-correlation plots obtained from the numerical simulations. Fig.5(a) and (b) indicates high-quality synchronization of the two PIC outputs when the feedback phases of the two PICs are matched. The cross-correlation value is 1.0 in Fig. 5(b). We thus numerically achieve common-signal-induced synchronization between the PICs with CARP light. In Figs. 5(c) and (d), the feedback phase of PIC 1 is shifted to 0.6 π. This parameter change affects the degradation of synchronization, and the cross-correlation value of two PICs is 0.038. These results are in good agreement with the experimental results in Fig. 3.

Figure 6 shows the numerical results of the fast Fourier transforms (FFT) of the temporal waveforms of the PIC outputs, corresponding to the RF spectrum of Fig. 4. In Fig. 6(a), both of the feedback phases of PICs are set to 0, and two peaks are observed and well matched in the FFTs as in the case of the experiment. On the contrary, when the feedback phase of PIC 1 is set to 0.6 π in Fig. 6(b), the peaks of the FFT of PIC 1 are shifted and mismatched to those of PIC 2. These results also agree with the experimental results in Fig. 4.

6. Conclusions

In conclusion, we experimentally achieved common-signal-induced synchronization in photonic integrated circuits driven by a constant-amplitude random-phase light. We obtained high cross correlation when the feedback phases of the PICs are matched. We investigate RF spectra of the PICs when the feedback phases are changed. Two RF spectra of the PICs are similar to each other when the feedback phases are matched. We also numerically investigated common-signal-induced synchronization of the PICs. The numerical results are in good agreement with the experimental results.

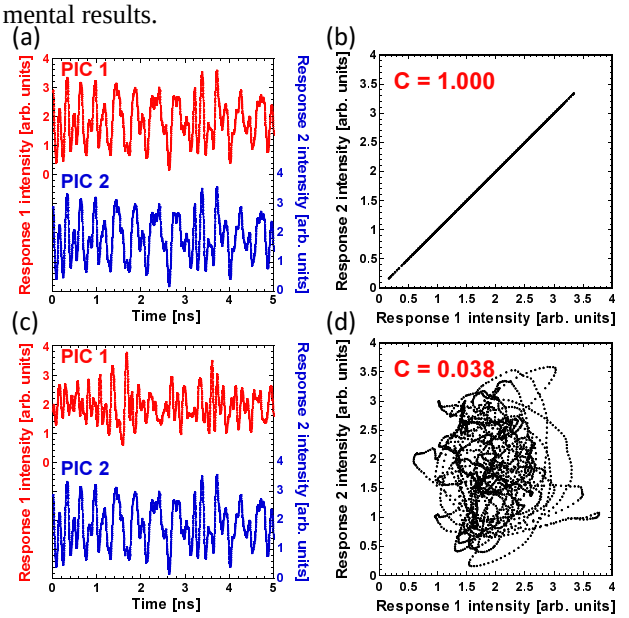

Figure 5: Numerical results of common-signal-induced synchronizaiton in two PICs. (a),(c) Temporal waveforms of PIC 1 and PIC 2, and (b),(d) correlation plots. The phases of the feedback lights are matched in (a),(b) and mismatched in (c),(d).

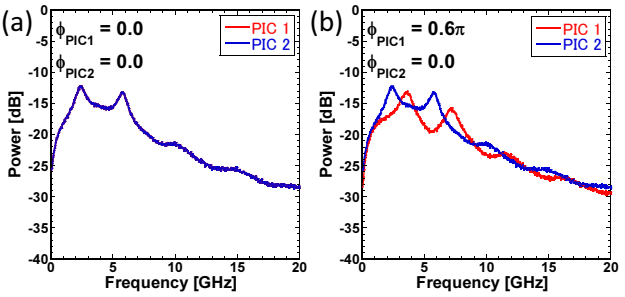

Figure 6: Numerical results of the FFTs of the PIC outputs. The feedback phases of PICs are (a) matched, and (b) mismatched.

Acknowledgments

We acknowledge support from Grants-in-Aid for Scientific Research from Japan Society for the Promotion of Science(JSPS KAKENHI Grant Number JP24686010), and Management Expenses Grants from the Ministry of Education, Culture, Sports, Science and Technology in Japan.

References

[1] C. E. Shannon, "Communication theory of secret system," Bell System Technical Journal, Vol. 28, pp. 656-

715 (1949).

[2] U. M. Maurer, "Secret key agreement by public discussion from common information," IEEE Transactions on Information Theory, Vol. 39, No. 3, pp. 733-742 (1993).

[3] J. Muramatsu, K. Yoshimura, K. Arai, and P. Davis, "Secret key capacity for optimally correlated sources under sampling attack," IEEE Transactions on Information Theory, Vol. 52, No. 11, pp. 5140-5151 (2006).

[4] J. Muramatsu, K. Yoshimura, and P. Davis, "Information theoretic security based on bounded observability," ICTTS 2009, Lecture Notes on Computer Science (LNCS), Vol. 5973, pp. 128-139, Springer, (2010).

[5] J. Muramatsu, K. Yoshimura, P. Davis, A. Uchida, and T. Harayama, "Secret-key distribution based on bounded observability," Proceedings of IEEE, Vol. 103, No. 10 pp. 1762-1780 (2015).

[6] K. Yoshimura, J. Muramatsu, P. Davis, T. Harayama, H. Okumura, S. Morikatsu, H. Aida, and A. Uchida, "Secure key distribution using correlated randomness in lasers driven by common random light," Physical Review Letters, Vol. 108, No. 7, pp. 070602 (2012).

[7] H. Aida, M. Arahata, H. Okumura, H. Koizumi, A. Uchida, K. Yoshimura, J. Muramatsu, and P. Davis, "Experiment on synchronization of semiconductor lasers by common injection of constant-amplitude random-phase light," Optics Express, Vol. 20, No. 11, pp. 11813-11829 (2012).

[8] H. Koizumi, S. Morikatsu, H. Aida, T. Nozawa, I. Kakesu, A. Uchida, K. Yoshimura, J. Muramatsu, and P. Davis, "Information-theoretic secure key distribution based on common random-signal induced synchronization in unidirectionally-coupled cascades of semiconductor lasers," Optics Express, Vol. 21, No. 15, pp. 17869-17893 (2013).

[9] K. Arai, K. Yoshimura, S. Sunada, and A. Uchida, "Synchronization induced by common ASE noise in semiconductor lasers," Proceedings of 2014 International Symposium on Nonlinear Theory and its Applications (NOLTA 2014), Vol. 1 pp. 474-477 (2014).

[10] K. Yoshimura, J. Muramatsu, A. Uchida, and P. Davis, "Spectral characteristics of consistency of a single-mode semiconductor laser injected with broadband random light," Proceedings of 2014 International Symposium on Nonlinear Theory and its Applications (NOLTA 2014), Vol. 1 pp. 545-548 (2014).

[11] R. Lang and K. Kobayashi, "External optical feedback effects on semiconductor injection laser properties," IEEE Journal of Quantum Electronics, Vol. 16, No. 3, pp. 347-355 (1980).